Functionalized xenon as a biosensor

Megan M. Spence*†, Seth M. Rubin*‡, Ivan E. Dimitrov§, E. Janette Ruiz*†, David E. Wemmer*‡, Alexander Pines*†¶, Shao Qin Yao‖, Feng Tian‖, and Peter G. Schultz‖**

*Department of Chemistry, University of California, Berkeley, CA 94720; †Materials Sciences and ‡Physical Biosciences Divisions, Lawrence Berkeley National Laboratory, Berkeley, CA 94720; §Department of Radiology, University of Pennsylvania, Philadelphia, PA 19104; and ‖Department of Chemistry and the Skaggs Institute for Chemical Biology, The Scripps Research Institute, 10550 North Torrey Pines Road, La Jolla, CA 92037

Contributed by Alexander Pines, July 17, 2001

The detection of biological molecules and their interactions is a significant component of modern biomedical research. In current biosensor technologies, simultaneous detection is limited to a small number of analytes by the spectral overlap of their signals. We have developed an NMR-based xenon biosensor that capitalizes on the enhanced signal-to-noise, spectral simplicity, and chemical-shift sensitivity of laser-polarized xenon to detect specific biomolecules at the level of tens of nanomoles. We present results using xenon ''functionalized'' by a biotin-modified supramolecular cage to detect biotin–avidin binding. This biosensor methodology can be extended to a multiplexing assay for multiple analytes.

Recent biosensor technologies exploit surface plasmon resonance (1), fluorescence polarization (2), and fluorescence resonance energy transfer (3) as detection methods. Although the sensitivity of such techniques is excellent, extending these assays to multiplexing capabilities has proven challenging because of the difficulty in distinguishing signals from different binding events. Although NMR spectroscopy is able to finely resolve signals from different molecules and environments, the spectral complexity and low sensitivity of NMR spectroscopy normally preclude its use as a detector of molecular targets in complex mixtures. Notable successes (4, 5) in the application of NMR to such problems are still limited by long acquisition times or a limited number of detectable analytes. Laser-polarized xenon NMR benefits from good signal-to-noise and spectral simplicity with the added advantage of substantial chemical-shift sensitivity.

Optical pumping (6) has enhanced the use of xenon as a sensitive probe of its molecular environment (7, 8). Laser-polarized xenon is being developed as a diagnostic agent for medical magnetic resonance imaging (9) and spectroscopy (10) and as a probe for the investigation of surfaces and cavities in porous materials and biological systems. Xenon provides information both through direct observation of its NMR spectrum (11–17) and by the transfer of its enhanced polarization to surrounding spins (18, 19). In a protein solution, weak xenon–protein interactions render the chemical shift of xenon dependent on the accessible protein surface and even allow the monitoring of the protein conformation (20). To use xenon as a specific sensor of molecules, it would be valuable to ''functionalize'' the xenon for the purpose of reporting specific interactions with a molecular target.

In this report, we demonstrate an example of such a functionalized system that exhibits molecular target recognition. Fig. 1 shows the chemical principle used for our initial study, a biosensor molecule designed to bind both xenon and protein. The molecule consists of three parts: the cage, which contains the xenon; the ligand, which directs the functionalized xenon to a specific protein; and the tether, which links the ligand and the cage. The ligand and target can be any two molecules or constructs. In such a molecule, it is expected that the binding of the ligand to the target protein will be reflected in a change of the xenon NMR spectrum.

Materials and Methods

Synthesis. Synthetic details of all cryptophane derivatives will be reported elsewhere in due course. Briefly, the cryptophane A-based biosensor molecule (shown in Fig. 1) was synthesized by a modified template-directed procedure (21). Starting from 3,4-dihydroxybenzaldehyde and using allyl bromide to reversibly protect the metahydroxyl group (22), one of the six methoxyl groups in cryptophane A was regioselectively replaced with a free hydroxyl group. On reacting with methyl bromoacetate followed by hydrolysis (23), the hydroxyl group in the modified cryptophane A was converted to a carboxylic acid, which was subsequently coupled (by using the 1-hydroxybenzotriazole hydrate (HOBt)/*o*-benzotriazol-1-yl-*N*,*N*,*N*′,*N*′-tetramethyluronium (HBTU)/*N*,*N*-diisopropylethylamine (DIEA) activation method) to the amino terminus of a protected short peptide CysArgLysArg on rink amide resin. The resulting cryptophane–peptide conjugate was deprotected and cleaved off the resin by using ''Reagent K'' (24), followed by purification with RP-HPLC [Microsorb (Rainnin) 80210C5, RP-C18 column, flow 4.5 ml/min, buffer A: 0.1% trifluoroacetic acid (TFA) in H_2O, buffer B: 0.1% TFA in CH_3CN, linear gradient from 40% to 80% buffer B in 30 min]. The purified conjugate was reacted with EZ-link TMPEO-Maleimide activated biotin (Pierce) to give the desired functionalized water-soluble cryptophane A, which was further purified by RP-HPLC (same conditions). The last two peptide conjugated-products were verified by matrix-assisted laser desorption/ionization (MALDI) time-of-flight mass spectrometry. All other intermediates were confirmed by ^{1}H NMR and MALDI–Fourier transform mass spectrometry.

Assay. The biosensor solution was prepared by dissolving ≈0.5 mg of the cryptophane derivative (molar mass 2,008 g mol^{-1}) in 700 μl of D_2O, yielding a concentration of ≈300 μM. This concentration was consistent with absorbance measurements at 284 nm (ε_{284} = 36,000 M^{-1}·cm^{-1}, determined for unmodified cryptophane-A by successive dilutions of a solution of known concentration). Approximately 80 nmol of affinity-purified egg white avidin (Sigma) was used without further purification. Natural abundance xenon (Isotec) was polarized and introduced to the sample by using previously described methods (16), showing ≈5% polarization. All NMR spectra displayed were obtained in single acquisition experiments at a nominal ^{129}Xe frequency of 82.981 MHz on a Varian Inova spectrometer. Only half of the sample was located inside the detection region, so spectra actually reflect detection of ≈40 nmol avidin monomer.

Results and Discussions

For the initial demonstration of this technique, biotin and avidin were chosen because of their high association constant (≈10^{15} M^{-1}) (25) and the extensive literature characterizing binding properties of modified avidin or biotin (26). The cage chosen for the prototype is a cryptophane-A molecule (21) with a polar peptide chain attached to make the cryptophane water soluble.

¶To whom reprint requests should be addressed. E-mail: pines@cchem.berkeley.edu.

**Present address: Departments of Chemistry and Biological Sciences, National University of Singapore, 3 Science Drive, Singapore 117543.

The publication costs of this article were defrayed in part by page charge payment. This article must therefore be hereby marked "*advertisement*" in accordance with 18 U.S.C. §1734 solely to indicate this fact.

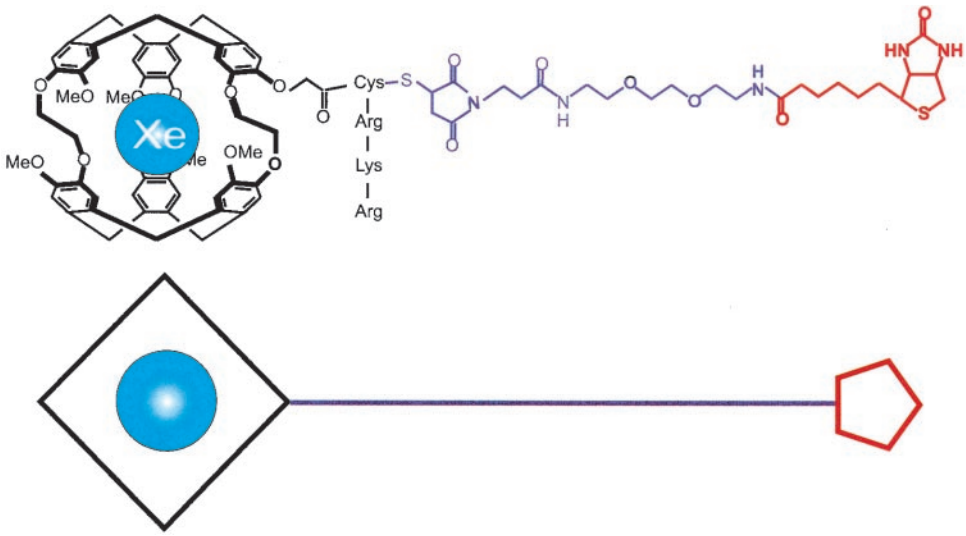

Fig. 1. Structure of a biosensor molecule designed to bind xenon to a protein with high affinity and specificity. The cage binding xenon, cryptophane-A, is shown in black; the ligand, in this case biotin, is shown in red; and the tether connecting them is shown in purple. The schematic representation of this structure is shown below.

Cryptophane-A has been shown to bind xenon with a binding constant K $\approx 10^3 \cdot M^{-1}$ in organic solvents (12), but the affinity is likely to increase in aqueous solution because of the hydrophobic nature of xenon. The characteristic chemical shift for xenon inside a cryptophane-A molecule is very unusual for xenon dissolved in solution, ≈130 ppm upfield from that of xenon in water. The only background xenon signal in the sample arises from free xenon in water, so the signal from the functionalized xenon is easily distinguishable. In the design of a xenon biosensor, a separate peak corresponding to xenon encapsulated by the

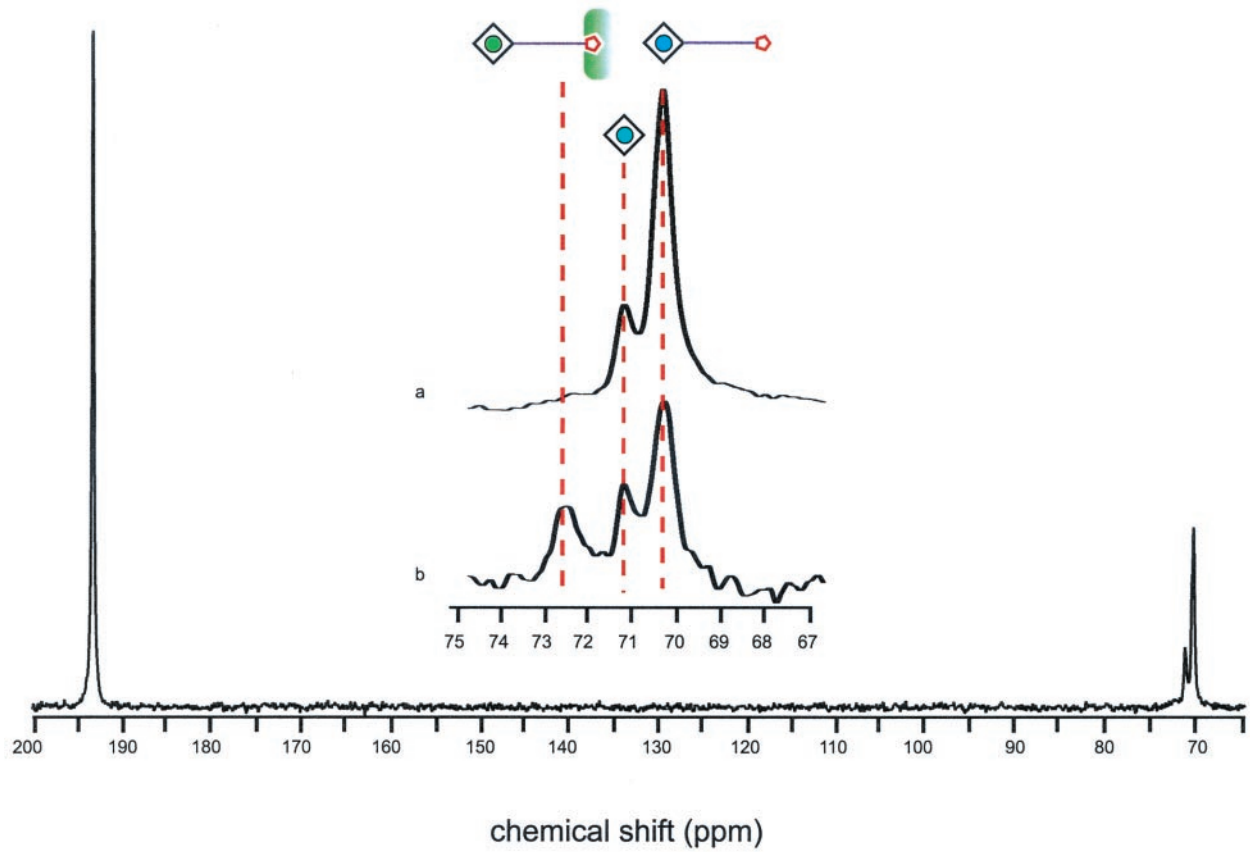

Fig. 2. Xenon-129 NMR spectra monitoring the binding of biotin-functionalized xenon to avidin. The spectrum of functionalized xenon in the absence of protein is shown in full, with the peak at 193 ppm corresponding to xenon in water, and peaks at 70 ppm corresponding to cryptophane-bound xenon. *Inset* shows only the cryptophane-bound peaks. *a* shows the functionalized xenon before the addition of avidin, with the more intense peak corresponding to functionalized xenon and the smaller peak corresponding to xenon in the cage without linker and ligand, serving as both a chemical shift and signal intensity reference. *b* shows the spectrum on the addition of ≈80 nmol of avidin monomer. A third peak, corresponding to functionalized xenon bound to avidin, has appeared, and the unbound functionalized xenon peak has decreased in intensity. All chemical shifts are referenced to that of xenon gas.

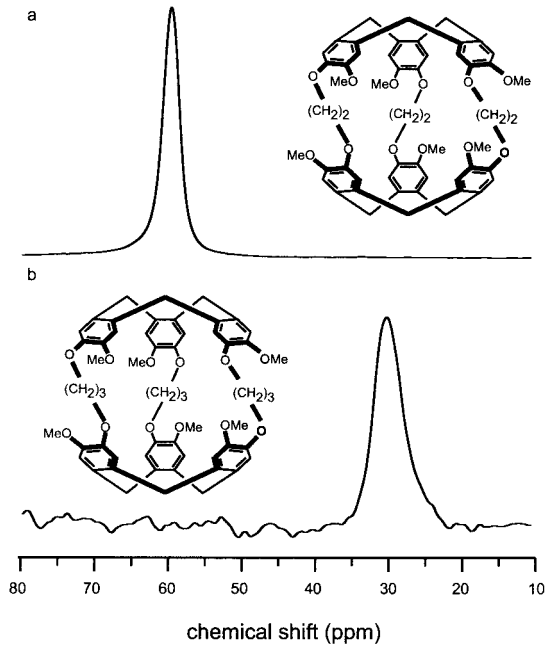

Fig. 3. Effect of cage structure on xenon chemical shift. *a* shows the chemical shift of xenon in cryptophane-A. *b* shows the chemical shift of xenon in a similar cage, cryptophane-E, a 30-ppm difference from that in cryptophane-A. The line widths for cryptophanes A and E are broadened by the exchange of xenon between the cage and tetrachloroethane, the organic solvent used.

cage is necessary, requiring both strong binding and a large difference between the xenon chemical shifts in the cage and solvent environments. The spin-lattice relaxation time for the functionalized xenon described here was measured to be greater than 40 s, sufficient time for the required transfer, mixing, and detection of the polarized xenon.

Fig. 2 shows the full ^{129}Xe NMR spectrum of the functionalized xenon in the absence of protein. The peak at 193 ppm corresponds to xenon free in water, whereas the peaks around 70 ppm are associated with xenon-bound cryptophane-A. These peaks are shown expanded in Fig. 2*a*, where the more intense upfield peak corresponds to functionalized xenon and has a linewidth of 0.15 ppm. A smaller peak ≈1 ppm downfield of the functionalized xenon peak is attributed to xenon bound to a bare cage, without linker and ligand. As the unfunctionalized caged xenon does not interact specifically with the protein, it serves as a useful reference for the chemical shift and signal intensity of the functionalized xenon in the binding event.

On addition of ≈80 nmol of avidin monomer, a third peak appears ≈2.3 ppm downfield of the functionalized xenon peak (Fig. 2*b*), attributable to functionalized xenon bound to the protein. Correspondingly, the peak assigned to free functionalized xenon decreases in intensity relative to the reference peak while its position remains unchanged. When the concentration of avidin is increased, there is a concomitant increase in the intensity of the third peak and a decrease in the peak corresponding to the unbound functionalized xenon (spectra not shown). As a control, avidin was saturated with biotin before the addition of the functionalized xenon to prevent binding of the functionalized xenon to the protein. When the functionalized xenon was added to the solution of biotin-saturated avidin, no downfield xenon peak was noted. Thus, the peak observable on the addition of avidin is an unambiguous identifier of biotin–avidin binding and hence the presence of avidin in the solution.

The mechanism of the chemical shift change on binding, currently being investigated, could result from actual contact between the cryptophane cage and the protein, leading to cage deformation and distortion of the xenon electron cloud. Changes in the rotational and vibrational motions of the cryptophane

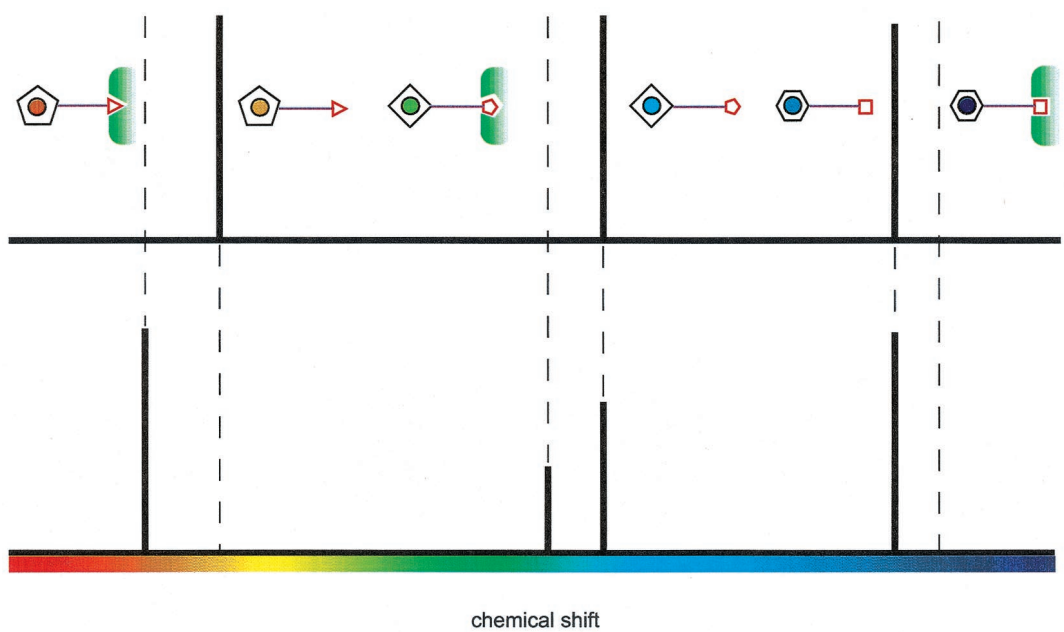

Fig. 4. Schematic diagram of one possible multiplexing scheme envisioned for functionalized xenon biosensors. The top spectrum shows the three distinct functionalized xenon peaks, corresponding to different cages linked to three ligands. The bottom spectrum shows the effect of adding the functionalized xenon to an unknown solution. On addition to the unknown solution, the leftmost peak shifts entirely, representing the case in which all functionalized xenon is bound to its corresponding protein. The central peak decreases in intensity, and a peak corresponding to the protein-bound functionalized xenon appears. The rightmost peak remains unaffected, indicating the absence of the corresponding protein target. The color of each xenon atom reflects its chemical shift in accordance with the color bar shown beneath the spectra.

cage caused by binding to the protein could also affect the xenon chemical shift. Xenon has long been used as a probe of cavity size, structure, and occupancy in microporous materials (14, 27–29). Indeed, the sensitivity of xenon to perturbations of the cage is so great that deuteration of one methyl group results in a readily discernible change in the bound xenon chemical shift (17).

The methodology that we have described offers the capability of multiplexing by attaching different ligands to different cages, forming xenon sensors associated with distinct resolved chemical shifts. As an example of this possibility, Fig. 3 shows the changes in bound xenon chemical shift caused by using different cages. The top spectrum is that of xenon bound to cryptophane-A in a tetrachloroethane solution, and the lower spectrum is that of xenon bound to cryptophane-E, analogous to cryptophane-A, but with an additional methylene group added to the bridges between the caps. The resulting bound xenon chemical shift is ≈30 ppm upfield from that of xenon bound to cryptophane-A. The diagram in Fig. 4 indicates schematically how we envision the possibility of a multiplexing protein assay. The binding event assays would be distributed over a large chemical shift range by attaching each ligand to a different cage. In the absence of the targeted proteins, the spectrum, depicted above, would consist of three resolved xenon resonances because of the effect on the xenon chemical shift caused by cage modifications. On binding each of the targeted proteins, the xenon peaks should shift independently, signaling each binding event and reporting the amount of protein present. As long as the differences in shift between xenon in the different cages exceed the shift change on binding, it should be possible to monitor and assign multiple binding events.

In conclusion, we have presented the concept for, and the initial implementation of, a biosensor that exploits the chemical shift of functionalized xenon on binding to an analyte. The approach has advantages over aspects of current biosensors, in that multiplexing assays and both heterogeneous and homogeneous assays should be possible. Furthermore, this methodology could be performed in biological materials *in vitro* or *in vivo* by combining the spatial encoding capabilities of MRI with the biosensing capabilities of the functionalized xenon. Potential targets include metabolites, proteins, toxins, nucleic acids, and protein plaques. Refinement of the functionalized detector molecules and the NMR procedures should enhance sensitivity by orders of magnitude relative to the experiments reported here.

M.M.S. and S.M.R. acknowledge the National Science Foundation and E.J.R. acknowledges Lucent Technologies/Bell Laboratories for predoctoral fellowships. I.E.D. received support from National Institutes of Health Grant RR02305. This work was supported by the Director, Office of Energy Research, Office of Basic Energy Sciences, Materials Sciences Division, Physical Biosciences Division, of the U.S. Department of Energy under Contract No. DE-AC03–76SF00098. This work was presented at 9th Chianti Workshop on Magnetic Resonance, Tirrenia, Italy, May 26–June 1, 2001.

1. Malmqvist, M. (1993) *Nature (London)* **361,** 186–187.
2. Checovich, W. J., Bolger, R. E. & Burke, T. (1995) *Nature (London)* **375,** 254–256.
3. Miyawaki, A., Llopis, J., Heim, R., McCaffery, J. M., Adams, J. A., Ikura, M. & Tsien, R. Y. (1997) *Nature (London)* **388,** 882–887.
4. Shuker, S. B., Hajduk, P. J., Meadows, R. P. & Fesik, S. W. (1996) *Science* **274,** 1531–1534.
5. Louie, A. Y., Huber, M. M., Ahrens, E. T., Rothbacher, U., Moats, R., Jacobs, R. E., Fraser, S. E. & Meade, T. J. (2000) *Nat. Biotechnol.* **18,** 321–325.
6. Walker, T. G. & Happer, W. (1997) *Rev. Mod. Phys.* **69,** 629–642.
7. Ratcliffe, C. I. (1998) *Annu. Rep. NMR Spectrosc.* **36,** 124–208.
8. Song, Y. Q., Goodson, B. M. & Pines, A. (1999) *Spectroscopy* **14,** 26–33.
9. Albert, M. S., Cates, G. D., Driehuys, B., Happer, W., Saam, B., Springer, C. S. & Wishnia, A. (1994) *Nature (London)* **370,** 199–201.
10. Wolber, J., Cherubini, A., Leach, M. O. & Bifone, A. (2000) *Magn. Reson. Med.* **43,** 491–496.
11. Tilton, R. F. & Kuntz, I. D. (1982) *Biochemistry* **21,** 6850–6857.
12. Bartik, K., Luhmer, M., Dutasta, J. P., Collet, A. & Reisse, J. (1998) *J. Am. Chem. Soc.* **120,** 784–791.
13. Luhmer, M., Goodson, B. M., Song, Y. Q., Laws, D. D., Kaiser, L., Cyrier, M. C. & Pines, A. (1999) *J. Am. Chem. Soc.* **121,** 3502–3512.
14. Springuel-Huet, M. A., Bonardet, J. L., Gedeon, A. & Fraissard, J. (1999) *Magn. Reson. Chem.* **37,** S1–S13.
15. Bowers, C. R., Storhaug, V., Webster, C. E., Bharatam, J., Cottone, A., Gianna, R., Betsey, K. & Gaffney, B. J. (1999) *J. Am. Chem. Soc.* **121,** 9370–9377.
16. Rubin, S. M., Spence, M. M., Goodson, B. M., Wemmer, D. E. & Pines, A. (2000) *Proc. Natl. Acad. Sci. USA* **97,** 9472–9475. (First Published August 8, 2000; 10.1073/pnas.170278897)
17. Brotin, T., Lesage, A., Emsley, L. & Collet, A. (2000) *J. Am. Chem. Soc.* **122,** 1171–1174.
18. Navon, G., Song, Y. Q., Room, T., Appelt, S., Taylor, R. E. & Pines, A. (1996) *Science* **271,** 1848–1851.
19. Landon, C., Berthault, P., Vovelle, F. & Desvaux, H. (2001) *Protein Sci.* **10,** 762–770.
20. Rubin, S. M., Spence, M. M., Dimitrov, I. E., Ruiz, E. J., Wemmer, D. E., Pines, A. (2001) *J. Am. Chem. Soc.*, in press.
21. Collet, A. (1987) *Tetrahedron* **43,** 5725–5759.
22. Kilenyi, S. N., Mahaux, J. M. & Vandurme, E. (1991) *J. Org. Chem.* **56,** 2591–2594.
23. Canceill, J., Collet, A., Gottarelli, G. & Palmieri, P. (1987) *J. Am. Chem. Soc.* **109,** 6454–6464.
24. King, D. S., Fields, C. G. & Fields, G. B. (1990) *Int. J. Pept. Protein Res.* **36,** 255–266.
25. Weber, P. C., Ohlendorf, D. H., Wendoloski, J. J. & Salemme, F. R. (1989) *Science* **243,** 85–88.
26. Wilchek, M. & Bayer, E. A. (1990) *Methods Enzymol.* **184,** 14–45.
27. Jameson, C. J., Jameson, A. K., Gerald, R. E. & Lim, H. M. (1995) *J. Chem. Phys.* **103,** 8811–8820.
28. Ripmeester, J. A. & Ratcliffe, C. I. (1995) *J. Phys. Chem.* **99,** 619–622.
29. Sozzani, P., Comotti, A., Simonutti, R., Meersmann, T., Logan, J. W. & Pines, A. (2000) *Angew. Chem. Int. Ed. Engl.* **39,** 2695–2698.